J. Plasma Physics (2002), *vol.* 68, *part* 5, *pp.* 321–330. © 2002 Cambridge University Press
DOI: 10.1017/S0022377802002039 Printed in the United Kingdom

Electron kinetics and selective ionization of recoil atoms in an ion guide ion source plasma

G. M. PETROV,[1] S. ATANASSOVA,[2] D. ZHECHEV,[2]
G. V. MISHINSKY[3] and V. I. ZHEMENIK[3]

[1]Berkeley Scholars Inc., PO Box 852, Springfield, VA 22150, USA

[2]Institute of Solid State Physics, Bulgarian Academy of Sciences, 72 Tzarigradsko Chaussee Blvd, BG-1784 Sofia, Bulgaria
(spectron@issp.bas.bg)

[3]Joint Institute for Nuclear Research, Flerov Laboratory of Nuclear Reactions, 141980 Dubna, Moscow Region, Russia
(laser@cv.jinr.ru)

(Received 1 November 2001)

Abstract. An electrodeless plasma produced in an ion guide ion source by a high-energy heavy ion beam propagating through a noble gas has been studied. The plasma parameters in Ar and He buffer gases have been calculated and analysed for projectile beam intensities from 10^9 to 10^{17} pps cm^{-2}. The plasma is characterized by very low electron and gas temperatures, but with an appreciable number of electrons with energy sufficient to ionize atoms of most chemical elements. The ion guide ion source plasma, combined with laser-enhanced ionization of the studied element, is used to improve the detection limit by enhancing the signal-to-noise ratio.

1. Introduction

The ion guide ion source (IGIS) technique is designed for investigating atoms and atomic nuclei far from the so-called β-stability line. Combined with resonant laser ionization (RLI) (Karnauhov 1978), IGIS provides detection of nuclear reaction products with a small cross-section and makes measurement in the millisecond lifetime range possible. The prospects of the IGIS technique and its independence of physical (half-life, recoil energy, etc.) or chemical characteristics are analysed by Deneffe and co-authors (Deneffe et al. 1987). The overall efficiency is measured to be within 0.1–2% (Morita et al. 1987; Yoshil et al. 1987; Taskinen et al. 1989). Dendooven gives a classification of different ion source concepts according to the way in which the reaction products are stopped (Dendooven 1997). The delay time distribution of the separated ions is measured to be broad, ranging from about 0.1 to 10 ms (Arje et al. 1986; Taskinen et al. 1989). The IGIS efficiency depends essentially on the plasma properties. The main plasma generation factor is a cyclotron charged particle beam, which ionizes the buffer gas atoms flowing through the IGIS cell. The beam creates extreme conditions inside the IGIS: a variety of elementary processes, lifetimes and particles: some with energies of the order of MeV. The yield of recoils can be enhanced by optimization of the IGIS plasma characteristics. So far there are few data on this type of plasma and

https://doi.org/10.1017/S0022377802002039 Published online by Cambridge University Press

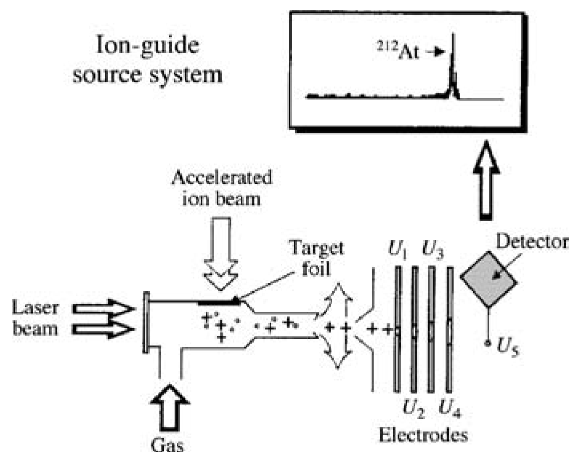

Figure 1. Measuring scheme – general view.

IGIS is considered as a *black box*, i.e. what is known is that the target input produces recoil nuclei and the detecting system output measures some number of recoil ions. In our opinion, the unique properties of the IGIS plasma are of significant interest, which motivated us to describe its properties quantitatively for a variety of input parameters.

In order to increase the signal-to-noise ratio, the IGIS plasma can be irradiated with a dye laser tuned to a suitable frequency in order to enhance the rate of collisional ionization of the analysed element. Excited atoms have a lower ionization potential compared with ground state atoms and are more efficiently ionized in collisions. The ionization rate coefficient in plasma with a Maxwellian electron energy distribution is governed by the so-called Arrhenius factor $\exp(-I_j/kT)$, where T is the plasma temperature, k is the Boltzmann constant, $I_j = I_0 - E_j$ is the ionization energy of the analysed atom in an occupied state j, I_0 and E_j are the ionization and excitation energy, respectively, accounted from the ground state. As a result, at an electron temperature of ~ 0.2 eV the ionization rate constant increases by two orders of magnitude per eV of optical excitation that moves the atom closer to its ionization limit (Travis et al. 1982).

The present paper aims to simulate the IGIS properties. The electron energy distribution function (EEDF) and the most important processes are analysed and discussed within the framework of possible experiments. The analysis includes solving the spatially averaged electron Boltzmann equation, accounting for ionization with a high-energy heavy ion beam and creation of secondary electrons. The results obtained will help to evaluate conditions favourable for laser-enhanced ionizations (LEI) in an IGIS environment.

2. Ion guide ion source

The operation of IGIS is based on the use of recoil ions, which are knocked out from a target by a projectile beam. The ions produced in such a way are stopped and transported by a gas flow through the exit hole to a vacuum chamber. Here the ions are separated from the buffer gas and usually directed to a mass-separator unit (Fig. 1). The main disadvantage of such a source is the strong dependence

https://doi.org/10.1017/S0022377802002039 Published online by Cambridge University Press

of the ion yield on the projectile intensity and charge. The yield, formed due to ionization of the buffer gas by the beam of projectiles, starts to decrease if the plasma density exceeds a certain optimum value, because the neutralization rate grows rapidly (the so-called *plasma effect*, Dendooven 1997). In general, the *plasma effect* limits the efficient application of IGIS. As a rule, IGIS is used only for producing nuclides in proton-induced reactions. However, multi-step multi-colour resonant laser ionization in a gas flow, used recently, made it possible to compensate for the decrease in ion yield as a result of their neutralization in a dense plasma (Kudryavtsev et al. 1996).

LEI in an IGIS plasma also allows one to circumvent the plasma effect. A continuous dye laser tuned to a suitable optical transition selectively excites recombined atoms of interest. As usual, the absorbing level is close to the continuum and enhances the probability of consequent ionization with thermal electrons. The chosen optical transition and atom–atom and atom–electron interactions in an IGIS medium determine the necessary degree of interatom selectivity and LEI efficiency. Therefore, the physical characteristics of IGIS are very important.

3. Main processes in IGIS

The cyclotron charged particle beam bombards the target on the inside surface of the IGIS. The projectiles penetrate into the IGIS and ionize the buffer gas atoms B, creating a specific medium, which differs from the known types of plasma. Unfortunately, little is known concerning this kind of medium. An IGIS medium consists of neutrals and ions of the buffer gas, electrons, recoil products and heavy projectiles losing their initial energy. The latter are continuously transferred from the highly energetic cyclotron projectiles to the other particles. The main part of this energy loss, $-dE/dx$, is ionization of buffer gas atoms. For projectiles with mass M and energy $E \ll \frac{M}{m_e} Mc^2$ the energy loss per unit length is

$$-\frac{dE}{dx} = \frac{4\pi n_e Z^2 e^4}{m_e v^2}\left[\ln\frac{2m_e v^2}{I} - \ln(1-\beta^2) - \beta^2 - \delta - U\right], \tag{1}$$

where e and m_e are the electron charge and mass, respectively; I is the ionization potential of the atom; n_e is the electron density in the target material; Z is the projectile charge; $\beta = v/c$ is the relative velocity v with respect to the speed of light c, and δ and U account for the influence of the density and the consistency of the K and L electrons. Thus the characteristics and behaviour of this kind of plasma follow those of particles B and B^+, and more specifically, the processes involving their ionization and recombination. A substantial part of the energy losses in (1) is transferred to the electrons, the energy of which is of importance for stepwise ionization as well as for describing the other properties of IGIS.

The EEDF is an essential part of the plasma kinetics. Knowledge of the EEDF is important for evaluating several plasma characteristics (electron density, mean energy, etc.) and to estimate the role of different elementary processes. The EEDF has been obtained by solving the time-independent and spatially averaged electron Boltzmann equation (Bretagne et al. 1982). The following processes have been accounted for: elastic scattering, excitation and ionization from the ground state of the buffer gas, diffusion, recombination and a source term describing the appearance of secondary electrons due to ionization by the fast ion beam. The solution method and the terms appearing in the electron Boltzmann equation are

https://doi.org/10.1017/S0022377802002039 Published online by Cambridge University Press

similar to an e-beam plasma, described in detail elsewhere (Bretagne et al. 1982). Only the ionization differential cross-section in the source term is different (since it describes ionization by an ion beam), for which an analytical formula derived by Garcia (1969) was used.

The EEDF $f(u)$ is calculated for a buffer gas pressure (He or Ar) of 100 torr, He^{++} projectiles with energy $E = 40$ MeV and intensity $I_{beam} = 10^9$–10^{17} pps cm^{-2} (particles s^{-1} cm^{-2}). The beam diameter is 1 cm and the gas target thickness is 1 cm. Under these conditions the production and loss of electrons in the IGIS buffer gas A have been calculated:

(i) ionization with ion beam projectiles

(ii) ionization with electrons

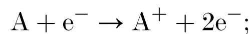

(iii) dissociative recombination

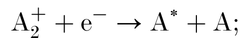

(iv) three-body recombination with an electron as a third particle

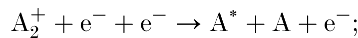

(v) three-body recombination with an atom as a third particle

electron diffusion to the wall.

4. Results and discussions

4.1. Electron macroscopic quantities

The EEDF has been calculated by solving the electron Boltzmann equation for energies of up to 100 eV. For larger kinetic energies the EEDF is negligibly small. The rate coefficients of all processes can be accurately described with the low-energy part of the EEDF. The EEDF and the other electron macroscopic quantities depend on several discharge parameters such as the buffer gas pressure and the beam intensity. The latter is of particular interest since it can be varied by orders of magnitude. Figures 2 and 3 show the EEDF at different beam intensities for He and Ar buffer gases, respectively. The EEDF in He consists of a Maxwellian distribution to up to kinetic energies of 1 eV, followed by a plateau between 1 and 20 eV (the elastic energy region) and a high-energy tail. The Maxwellian part is independent of the beam intensity, while both the plateau and the high-energy tail of the EEDF depend on the beam intensity. This dependence is, however, not very prominent: approximately proportional to the square root of the beam intensity. For an Ar buffer gas the Maxwellian distribution extends up to kinetic energies of 2 eV. The different behaviour of the EEDF in the elastic energy region in the Ar buffer gas (Fig. 3) compared with He buffer gas (Fig. 2) is a result of the different momentum transfer cross-section for elastic electron–atom collisions.

At low beam intensity the temperature of the bulk electrons is $T_e = 300$ K (Fig. 4). For beam intensities exceeding 10^{12} pps cm^{-2} projectiles transfer a sufficient amount of energy to the electrons and the temperature of the bulk electrons

https://doi.org/10.1017/S0022377802002039 Published online by Cambridge University Press

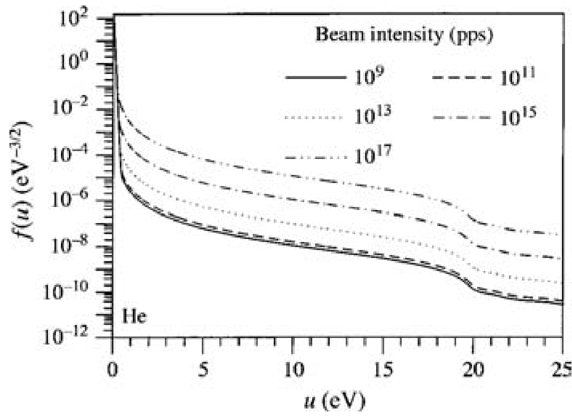

Figure 2. EEDF in He buffer gas at various beam intensities.

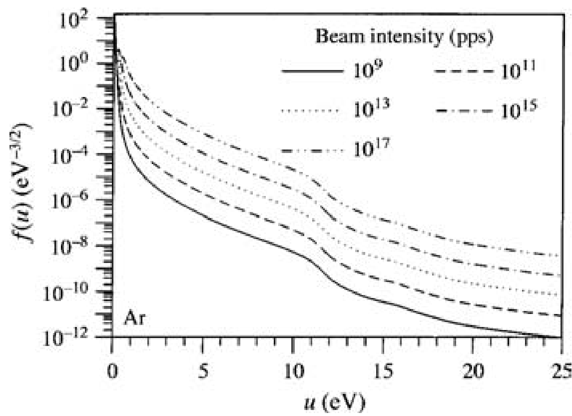

Figure 3. EEDF in Ar buffer gas at various beam intensities.

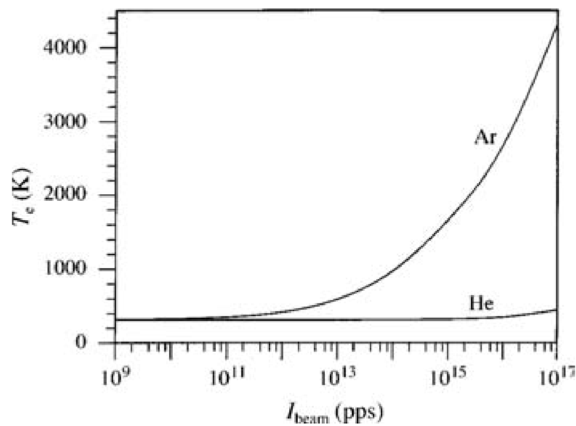

Figure 4. Electron temperature versus beam intensity.

https://doi.org/10.1017/S0022377802002039 Published online by Cambridge University Press

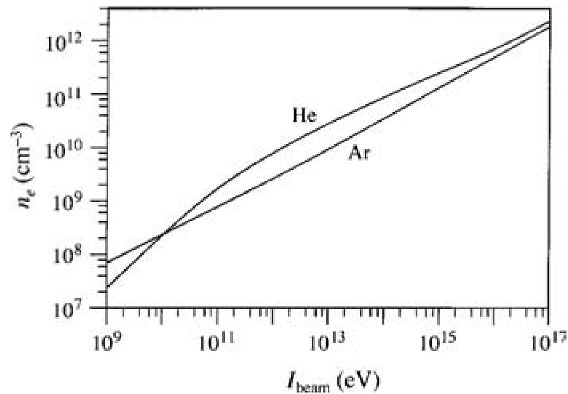

Figure 5. Electron density versus beam intensity.

exceeds the gas temperature, if Ar is used as a buffer gas. The electron temperature gradually increases with the beam intensity, approaching 0.4 eV at a beam intensity of 10^{18} pps cm^{-2}. In a He buffer gas the electron temperature remains at 300 K even at very high beam intensities. Elastic collisions with He are very efficient due to the large momentum transfer cross-section and the small mass ratio, and the high power loss in elastic collisions keeps the electron temperature equal to the gas temperature (300 K). It should be noted, however, that in spite of the low temperature of the bulk electrons they are still capable of exciting and ionizing the buffer gas atoms due to the high-energy tail of the EEDF. Except for this unusually low electron temperature, the plasma under investigation resembles the EEDF in an electron-beam-generated plasma in many respects.

An increase in the beam intensity inevitably leads to a proportional increase of the ionization rate and consequently to an increase of the electron density (Fig. 5). The latter is nonlinear since it depends on the interplay between different processes, which will be further analysed. Owing to the high bound energy of the valence electrons, the buffer gas is predominantly ionized by heavy projectiles. The electrons also contribute to ionizations, but to a much smaller extent. Electrons account for about 22% of the total number of ionizations for Ar and about 8.5% for He. The electron loss processes are diffusion and recombination. Figures 6 and 7 illustrate the contribution of various recombination processes and diffusion to the electron loss for He and Ar buffer gas, respectively. The diffusion losses in an Ar buffer gas are negligible. In a He buffer gas the electron loss through diffusion is the dominant loss channel for beam intensities of up to 10^{11} pps cm^{-2}, but at higher beam intensities the electron density increases and the recombination becomes the major electron loss channel.

The lifetime of free electrons also depends on the electron loss mechanism. In He, for example, it is independent of the beam intensity, provided the latter is less than 10^{11} pps cm^{-2} (Fig. 8). When the recombination becomes the dominant loss channel, the lifetime decreases dramatically. This may be important for understanding the 'plasma effect' in IGIS (Dendooven 1997). It is much easier to analyse the lifetime of electrons in Ar. Since dissociative recombination dominates regardless of electron density, the electron lifetime is inversely proportional to electron density. At very high beam intensity it is of order of a few microseconds.

https://doi.org/10.1017/S0022377802002039 Published online by Cambridge University Press

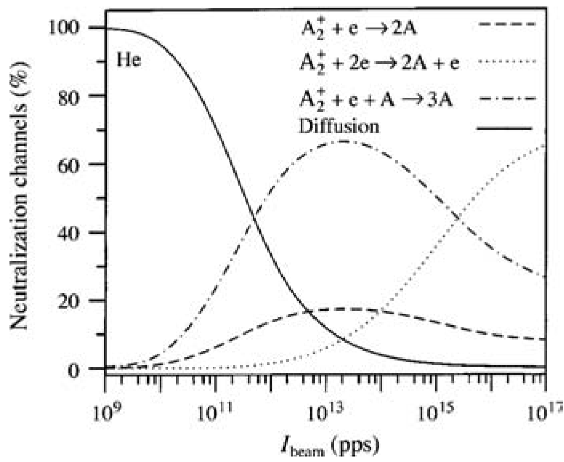

Figure 6. Neutralization channels in He buffer gas versus beam intensity.

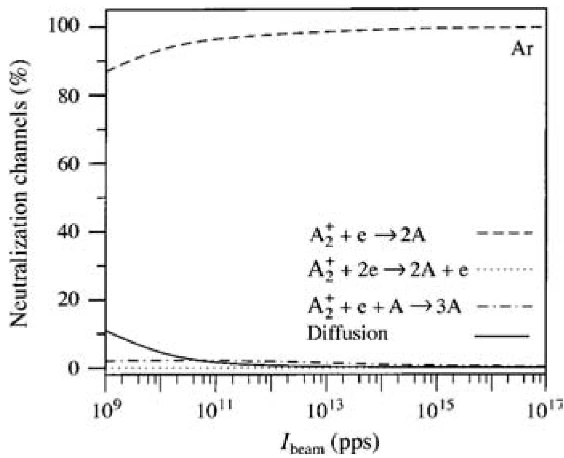

Figure 7. Neutralization channels in Ar buffer gas versus beam intensity.

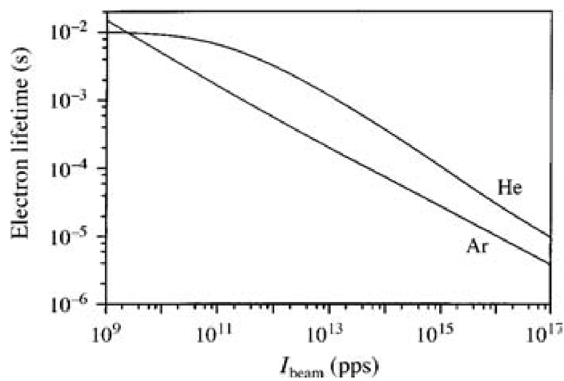

Figure 8. Electron lifetime versus beam intensity.

https://doi.org/10.1017/S0022377802002039 Published online by Cambridge University Press

Table 1. Calculated values of α_0 for atoms with ionization energy I_j of 4 and 2 eV in the excited state and 6 eV in the ground state.

I_j	α_0		
	He	Ne	Ar
4 eV	2.9	4.0	7.7
2 eV	11.5	22.9	98.1

4.2. Selective ionization of analysed atoms in IGIS

What signal-to-background ratio may be expected in selective laser excitation of recoil atoms in IGIS? A laser usually excites an atom to a level close to the ionization potential. Electron impact ionization dominates for such atoms in a dense plasma. According to Gryzinski (1965) and Deutsch and Mark (1987), Thomson's classical expression for the single-ionization cross-section σ_j near the ionization threshold may be written as

$$\sigma_j = 4\pi r^2 N \frac{R}{I_j t}\left(\frac{t-1}{t+1}\right)^{3/2}\left\{1+\frac{2}{3}\left(1-\frac{1}{2t}\right)\ln\left[2.7+(t-1)^{1/2}\right]\right\}, \tag{2}$$

where r is the mean square radius of the outer electron sublevel possessed by the atomic state; N and I_j are the number of electrons and ionization energy in the valence subshell, respectively; R is the Rydberg constant; $t = E/I_j$ is the kinetic energy relative to the threshold and E is the energy of the incident electron.

Let us analyse the ionization of an atom with one valence electron and two energy levels only – ground state 0 and excited state 1. The ionization rate coefficient k_j for the atom in state j is defined as

$$k_j = \int_{I_j}^{\infty} \sigma_j(E)\mathbf{v}(E)\sqrt{E}f(E)\,dE, \tag{3}$$

where $\mathbf{v}(E)$ is the velocity of the incident electron. The ionization rate coefficient for the atom in an excited state is significantly larger compared with that for the atom in a ground state. The ratio of the ionization rate coefficients for excited and ground state atoms can be written as $\alpha = k_1/k_0 = \alpha_0(r_1/r_0)^2$, where r_0 and r_1 are the radii of the outer electron subshells for the ground and excited states, respectively; and α_0, according to our calculation, is almost independent of the projectile intensity, but depends strongly on the nature of the buffer gas. Table 1 presents the calculated values of α_0 for atoms with ionization energy in a ground state of 6 eV and in an excited state of 4 or 2 eV, which suggests that Ar is much more suitable as a buffer gas for LEI compared with He and Ne. This can be a cause of discouraging results such as the experiments of Campbell et al. (1998), who did not see any change in ion yield, using He as the buffer gas and Sr as the element under investigation.

If we neglect the ionization by heavy projectiles, the ratios of the populations of excited and ground state atoms in the presence (ξ) and in the absence (ξ_0) of laser radiation are as follows:

$$\xi = \frac{B_{01}E_v + k_{01}}{B_{10}E_v + A_{10} + k_{10}} \tag{4a}$$

$$\xi_0 = \frac{k_{01}}{A_{10} + k_{10}}, \tag{4b}$$

https://doi.org/10.1017/S0022377802002039 Published online by Cambridge University Press

where B_{01}, A_{10} and B_{10} are the Einstein coefficients for absorption, emission and stimulated emission; k_{01} and k_{10} are the collision rate coefficients for excitation and de-excitation of the upper level, respectively; E_ν is the laser spectral irradiance. The ionization rate from level j is equal to $k_j N_j$, where N_j is the number of atoms at level j. In the two-level atom approximation for a laser-irradiated plasma, the ionization degree of the analysed element $S = \frac{n_i}{n_i + n_a}$, where n_i and n_a are the number of ions and neutral atoms, respectively (here we neglect the formation of chemical compounds with contamination atoms and buffer gas ions, charge exchange, etc.) reaches the value

$$S = \frac{S_0 \beta}{1 + S_0(\beta - 1)}, \tag{5}$$

where S_0 is the ionization degree in the absence of laser radiation and $\beta = \frac{(1+\xi_0)(1+\alpha\xi)}{(1+\xi)(1+\alpha\xi_0)}$ is the relative increase of the ionization rate due to laser irradiation. In the case of optical transition saturation $\xi = B_{01}/B_{10} = g_1/g_0$, where g_0 and g_1 are the statistical weights of the ground and excited states, respectively. If we assume that $\xi_0 \ll 1$, then β cannot exceed the value $\frac{\alpha g_1 + g_0}{g_1 + g_0}$, which is equal to $(\alpha + 1)/2$, when $g_1 = g_0$. If we assume that $\beta = 20$, then for $S_0 = 1\%$ we can expect S to grow up to 17% and for $S_0 = 10\%$ to grow up to 70%. Such growth can significantly improve the IGIS efficiency.

5. Conclusions

An electrodeless plasma produced in IGIS by a heavy ion beam propagating through a noble gas has been studied. The EEDF in Ar and He buffer gases for an IGIS plasma medium has been calculated. In a He buffer gas the EEDF consists of a Maxwellian distribution with $T_e \approx T_g = 300\,\mathrm{K}$ and a high-energy tail. The tail of the EEDF is almost independent of the projectile beam intensity of up to 10^{11} pps cm^{-2}. In spite of the low mean electron energy, the IGIS plasma contains electrons with energy sufficient to ionize atoms of most chemical elements. The electron density and temperature are estimated to be 10^7–10^{12} cm^3 and 300–4000 K, respectively, depending on the ion beam intensity. The contribution of the different neutralization channels for electrons is calculated for this type of plasma medium.

The possibility of LEI in IGIS was demonstrated and its distinction from conventional EFI is analysed. The proposed technique allows IGIS to operate in the element selective mode. This source also allows one, where it is possible, to obtain information concerning the isotope shift of an optical transition.

References

Arje, J., Aysto, J., Hyvonen, H., Taskinen, P., Koponen, V., Honkanen, J., Valli, K., Hautojarvi, H. and Vierinen, K. 1986 *Nucl. Instrum. Meth. Phys. Res.* **A247**, 431.

Bretagne, J., Godart, J. and Puech, J. 1982 *J. Phys. D: Appl. Phys.* **15**, 2205.

Campbell, P. et al. 1998 *Proc. 3rd Int. Workshop on Application of Lasers in Atomic Nuclei Research, Poznan, Poland* 1997 Dubna, E15-98-57, p. 44.

Dendooven, P. 1997 *Nucl. Instrum. Meth. Phys. Res.* **B126**, 182.

Deneffe, K., Brus, B., Coenen, E., Gentens, J., Huyse, M., van Duppen, P. and Wouters, D. 1987 *Nucl. Instrum. Meth. Phys. Res.* **B26**, 399.

Deutsch, H. and Mark, T. D. 1987 *Int. J. Mass Spectrosc. Ion. Proc.* **70**, R1.

Garcia, J. D. 1969 *Phys. Rev.* **177**, 223.

https://doi.org/10.1017/S0022377802002039 Published online by Cambridge University Press

Gryzinski, M. 1965 *Phys. Rev.* **138**, 336.

Karnauhov, V. A. 1978 Internal Report, Dubna, p.13.

Kudryavtsev, Yu. et al. 1996 *Nucl. Instrum. Meth. Phys. Res.* **B114**, 350.

Morita, K. et al. 1987 *Nucl. Instrum. Meth. Phys. Res.* **B26**, 406.

Taskinen, P., Pentila, H., Aysto, J., Dendooven, P., Jauho, P., Yokinen, A. and Yoshil, M. 1989 *Nucl. Instrum. Meth. Phys. Res.* **A281**, 539.

Travis, J. C., Turk, G. C. and Green, R. B. 1982 *Anal. Chem.* **54**, 1006A.

Yoshil, M., Hama, H., Taguchi, K., Ishimatsu, T., Shinozaka, T., Fujioka, M. and Arje, J. 1987 *Nucl. Instr. Meth. Phys. Res.* **B26**, 410.

https://doi.org/10.1017/S0022377802002039 Published online by Cambridge University Press